

DOI: <https://doi.org/10.24297/jap.v24i.9872>**Prototyping of Self-Sufficient Marine Propulsion Systems**

Ramon Ferreiro Garcia

Former Prof. Emeritus at the Industrial Eng. Dept., University of A Coruna Spain

(Received: Month / Year. Accepted: Month / Year)

Abstract

This work presents the development of a marine propulsion system with a net-zero emissions energy supply. While the final propulsion element remains a conventional propeller or water-jet, the primary innovation lies in its power source. The main challenge is to create an energy supply that is not only carbon-neutral, but also self-sufficient, viable, and reliable. To achieve this, we propose a disruptive shift: replacing conventional fossil-fuel engines with a Self-Sufficient Power Machine (SSPM). This disruptive approach eliminates the need for traditional fuel storage and allows autonomous vessels to integrate SSPM-based resources for powering all services, including critical systems. Since it requires no fossil fuel or any other type of fuel, it offers unlimited autonomy. This advantage is essential for submarines and other submersible vehicles.

The results, based on a generic case study with seven cascaded power units operating at temperatures between 300 and 1000 K, confirmed the following regarding self-sufficiency: The calculated net positive output of 1513 kJ/kg-cycle after considering feedback heat demonstrates the system's ability to maintain its own operation while generating a significant amount of free work.

Keywords: Self-Sustaining Power Generation, Cascaded Coupled Power Units, Constant Temperature Drop, Vacuum-Induced useful work, Thermodynamic Disruption.

Nomenclature related to general sVsVs cycles and SSPG

Acronyms	Description/Context
Cont, cont	Subscript of contraction process: A form of compression (volume decrease) achieved by cooling a TWF, which generates a pull force while increasing internal energy and pressure.
CTF	HTF for cooling: Cooling Transfer Fluid (conventionally, thermal oil)
E_i	Energy input (heat and/or work)
EM	Electromagnetic
E_o	Energy output (heat and/or work)
EP	Electric Power
TEP	Total real or effective electric power (the effective generator output power)
NEP	Net electric power: $NEP = TEP - q_{i_feedback}$ (available useful EP)
Exp, exp.	Subscript of expansion process: A form of expansion (volume increase) achieved by heating a TWF, which generates a push force while decreasing internal energy and pressure.
FCF	Forced convection fan (recirculation fan of the TWF)
FP	Feed pump (feed compressor of the TWF)
Gen	Electric Power Generator: alternator or generator
H, L	Subscript of High, Low: i.e. T_L with L subscript of T_{low} , T_H , with H subscript of T_{high}
HTF	Heating Transfer Fluid (conventionally, liquid as thermal oil or gas as H_2)
Is_{eff}	Isentropic efficiency: (open processes). losses factor inherent to real gas exp/comp.
LF	Losses factor (include thermo-mechanical and thermo-hydraulic losses)
MPS	Marine Propulsion System
PU	Power Unit driven by the thermal cycle sVsVs or VsVs cycle
$q_{i_feedback}(PU1)$	Electric power as heat added to the first cascaded PU. $q_{i_elect_PU1} = (h_2 - h_1)$ of PU1
RF	Heat recovery factor (heat transfer losses including heat leaks)

sp	State point of any stationary point state of a thermal cycle
SSPM	Self-Sustaining Power Machine, Self-Sufficient Power Machine
SSPG	Self-Sustaining Power Generator, Self-Sufficient Power Generator
Suct, suct.	Subscript of suction process: A form of expansion (volume increase) achieved by adding useful work to the system by means of a pull force, while decreasing internal energy and pressure.
TWF	Thermal Working fluid (a gas with high adiabatic expansion coefficient such as helium or argon)
sVsVs	sequential processes of the cycle sVsVs: Isentropic s , Isochoric V , adiabatic s , Isochoric V , adiabatic s : [sVsVs]
TF (%)	Heat transfer losses due to heat recovery effectiveness
LF (%)	Losses factor (thermal and mechanical irreversibilities)
η_{th} (%)	Cycle thermal efficiency [w_n/q_i]
Symbols/units	description
p (bar)	pressure
q_i (kJ/kg)	specific heat in to a cycle process
q_{i23} (kJ/kg)	Input heat to cycle process 2-3
q_o (kJ/kg)	specific heat out from a cycle process
q_{o4-5} (kJ/kg)	output heat from cycle process 4-5 in a sVsVs cycle
q_{rec}	Recovered heat from cycle process 4-5 in every sVsVs cycle-based PU
C_p (kJ/kg-K)	specific heat capacity at constant pressure
C_v (kJ/kg-K)	specific heat capacity at constant volume
s (kJ/kg-K)	specific entropy
S_{sys} (kJ/kg-K)	specific entropy of a thermodynamic system
S_{surr} (kJ/kg-K)	specific entropy of the surroundings of the system
S_{gen} (kJ/kg-K)	specific entropy generated in a thermodynamic process
h (kJ/kg)	specific enthalpy; $h=C_p \cdot T$; $T=f(T)$
T (K)	Absolute temperature
T_H (K)	top cycle temperature
T_L (K)	bottoming cycle temperature
u (kJ/kg)	specific internal energy
v (m ³ /kg)	volume
V (m ³)	specific volume
w (kJ/kg)	specific work
w_i (kJ/kg)	specific work input
$w_{i12} = w_{iFP}$	Input work to the Feed Pump: $w_{iFP} = \Delta h_{12} = h_2 - h_1 = C_p \cdot (T_2 - T_1)$
w_o (kJ/kg)	specific work out
w_{oexp} (kJ/kg)	Output expansion work due to previously added heat
w_{ocont} (kJ/kg)	Output contraction work due to previously extracted heat
w_{oexp34} (kJ/kg)	Output expansion work w_{o34} due to previously added heat
$w_{ocont51}$ (kJ/kg)	Output contraction work w_{o51} due to previously extracted heat
w_n (kJ/kg)	Net useful work ($w_{oexp} + w_{ocont}$) = ($w_{o34} + w_{o51}$) in an VsVs thermal cycle
q_{rec}/PU_i (kJ/kg)	Heat recovered from every PU from cooling cycles processes
η_{th} (%)	Cycle thermal efficiency (w_n/q_i)

1. Introduction

Global shipping consumes approximately 300 million tones of fuel annually [1], accounting for roughly 3% of global anthropogenic emissions and about 7-10% of total transport-related energy consumption. The sector

relies heavily on heavy fuel oil, marine gas oil, and natural gas, with emissions expected to rise significantly without further regulation.

The amount of CO₂ emitted annually by industry in general, and maritime transport in particular, is significant enough to justify a paradigm shift in the use of technologies and services for both industrial production and propulsion, including their associated services. Fortunately, a disruptive, innovative, and environmentally friendly technological solution has been developed to mitigate and ultimately eliminate this problem. Given the availability of these technologies, it can be implemented at reasonable costs.

1.1 The Proposed Solution

Based on the comments and data above, the consequences of emissions, which unfortunately tend to increase, are too high and costly. The preceding comment reveals the imminent need for a truly disruptive decision: a radical shift in the energy paradigm worldwide that affects the fundamental principles of thermodynamics; obtaining work through vacuum-induced thermal contraction, achieved by cooling or heat extraction; that is, useful mechanical work is performed by extracting heat rather than adding it. The rate of useful work obtained through thermal contraction achieved by cooling-induced vacuum can ultimately approximate the amount of useful work obtained by adding heat. In fact, it represents almost twice the amount of work relative to the heat added.

To mitigate these risks and their consequences, a disruptive paradigm shift is proposed: replacing conventional fossil fuel-based Marine Propulsion Systems (MPS) with self-sustaining thermoelectric power plants capable of supplying energy without incurring any of the risks associated with fossil fuel-based energy. The proposed techniques do not require fossil or nuclear fuels, or any other fuel that requires combustion. They are technically feasible and cost-effective.

The reason this principle hasn't been applied earlier, that is, at the beginning of the industrial era more than two centuries ago (when the fundamental principles of thermodynamics were formulated), is due to the neglect of elementary physical concepts. This is probably because the solution adopted was based on heat transfer from a given potential to a lower one to produce work through adiabatic expansion, without considering other possible principles such as reverse heat transfer—from lower to higher temperatures—which gives rise to work by thermal contraction, one of the fundamental pillars of this proposal.

This technique leads to a reconsideration of the energy balances that affect the first law of thermodynamics and exergy, or available useful energy. This is only due to the effect of the vacuum-induced useful contraction work, which accounts for the energy balance without the necessity of added heat, or in other words, this is solely due to the effect of the useful contraction work induced by the vacuum, which explains the energy balance without the need for added heat. This phenomenon violates the conventional fundamental principles of physics, especially thermodynamics, including quantum fundamentals.

1.2 The Self-Sustaining Power Machine

The concept of Self-Sustaining or Self Sufficient Power Machines or (SSPMs) has been introduced and described in previous references [4-7] , [10-12] and patents [15-19]. In short, it consists of a disruptive, technically and economically viable alternative solution that allows for the in situ intensive generation and supply under demand or dissipation of heat to the environments.

1.3 The proposed power units based on Pulses-based Gas Turbines [6], Patent [20]

The proposed SSPM is composed by a cascade of PUs. Every PU consists of a disruptive Self-Sustaining Power Machine (SSPM) composed of cascaded power units (PUs). Each PU consists of a Pulse Gas Turbine (**PGT**). The prototyping design task involves a singular thermal cycle (sVsVs) associated to each PU, characterized by doing useful work by in the same way as the known VsVs cycle. The main characteristics of the sVsVs cycle responsible for driving each of the PUs of an SSPM include:

- (a) Adiabatic expansion of a Thermal Working Fluid (TWF) due to previous heat addition,
- (b) Adiabatic contraction of a TWF previously cooled by heat extraction and, [2-3]

- (c) Upgrading recovered heat by increasing thermal potential by heat superposition techniques, and
- (d) Efficient use of the heat recovered from each upstream PU to feed the first PU downstream.

The fact of achieving useful mechanical work with the above-mentioned procedures by adding only heat to produce expansion work undergoes an excess of useful mechanical work greater than the amount of added heat, which gives rise to a SSPM enabled to defy Perpetual Motion Machines (PMM) of second kind.

In the proposed configuration, the heat released from each PU due to the cooling of the TWF is efficiently recovered and reused in the first PU in the cascade. Results have been verified through two case studies carried out on a SSPM simulated prototype [6], being conducted using air and helium as real gases.

The significant differences of the presented technology based on the proposed PGT technology [6], compared to Rankine, ORCs, and Brayton cycles used in the most advanced power plants are summarized in the following points:

There are no phase changes of the TWF (such as helium, dry nitrogen, dry air, among other TWFs, which means that the heats of vaporization and condensation are not present.

The tasks of adding and extracting heat to/from the cycle are carried out at constant volume. This is possible by alternately operating with two or more heating and cooling isochoric reservoirs, which operate under forced convection heat transfer.

No conventional feed pumps are required because there are no phase changes. Instead, a low-pressure TWF feed compressor is used, where the low-pressure compression is due to the fact that during the time the working fluid is being pumped from a low-temperature fluid reservoir to a high-temperature fluid reservoir, it exhibits suction and discharge pressures very close to each other.

Cooling turbine blades is not required in any case.

An installation based on a cascade coupling structure of a group of PGTs with respect to the heat transfer fluid (HTF) temperature mechanically coupled on the same rotating shaft contributes to an effective waste heat recovery system based on the following facts:

- 1 Effective recovering and use of low-grade heat exhausted from the connected upstream turbines.
- 2 The thermal efficiency of a PGT cycle is independent of the range between high and low temperatures since it does not obey Carnot constraints. Contrary to Carnot, indeed, efficiency is higher for low-temperature ranges ($T_H - T_L$) which implies high temperature ratios (T_L/T_H). This characteristic also contributes to the increase of the residual heat utilization factor.

Given that the efficiency of each individual PGT is significantly higher than in conventional Rankine cycles-based steam turbines, associated to the fact that the heat utilization factor is also greater, the overall efficiency is significantly increased.

In summary, the key innovations and contraction, the efficient recovery and reuse of contraction heat, and the strategic selection of the TWF and number of PUs, consist of the utilization of thermal contraction to generate work, the specialized thermal cycles that leverage expansion working fluids - all of which contribute to the SSPM's remarkable improvements in thermal efficiency and self-sufficiency. Consequently, the proposed power and propulsion architecture presents characteristics that challenge the most advanced technologies including modern nuclear reactors.

By not using any type of fuel, a list of equipment, associated tasks, and some drawbacks cease to exist, among which the following stand out:

--fuel tanks

--fuel refueling facilities

--fuel treatment tasks for combustion

--refueling tasks and associated time

--no space and weight associated with fuel tanks

--costs associated with fuel consumption.

1.4 Purpose & Roadmap

With the aim of providing technical means for energy supply to assist all types of industrial activities in all areas associated with the marine transport, the following sections will describe two key topics: energy self-sufficiency and propulsion for marine transport. Therefore, the work is organized according to the following structure: Section 2: Modeling of an SSPM with cascaded pulse gas turbines, based on references [2-12] and [13-18]. Section 3: Modeling of the ship's propulsion system. Section 4: Analysis of results. Section 5: General conclusions and implications.

2. Modeling a SSPM with cascaded Pulse-based Gas Turbines

The proposed marine propulsion-based SSPM consist of a set of cascaded power units made up of gas turbines operating on barothermal impulses (PGT) driven by known thermal cycles of the sVsVs type [6], [20]

2.1 Brief Description of the PGT Structure and its Operating Modes

The Power Generation Units (PUs) for the proposed Self-Powered Power Plant (SPPP) prototype are based on the PGT (Pulsed Gas Turbine) technology patented under application number P202000032 and publication number ES2851381. The PGT scheme is illustrated in Figure 1a.

The PGT structure is composed at least of four main subsystems:

- Heat supply system, responsible for heating the thermal working fluid (TWF) which gives rise to puss forces enabled to do useful expansion work,
- Heat extraction system, responsible for cooling the TWF which gives rise to a vacuum responsible for pull forces enabled to do useful contraction work,
- Heat recovery system enabled to recover the cooling heat released from the heat extraction system which will be feed back to the internal heat supply system,
- Pulse-based gas turbines (PGT) itself,
- Thermal working fluid pump feeding system,
- Systems circuits and controlled valves and, - advanced control equipment.

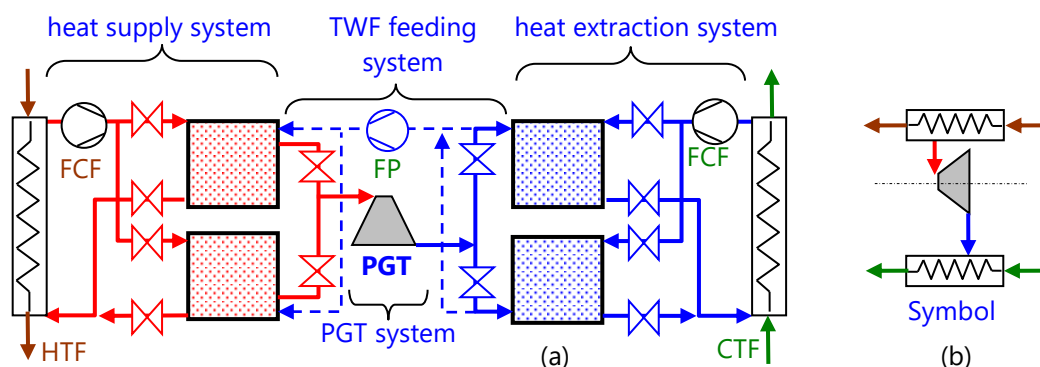


Figure 1: Illustration of the PGT based on the patent application number P202000032 and publication number ES2851381, [16], [20]. Figure 1(a) depicts the main subsystems including the heat supply system, the heat extraction system, the TWF feeding system and the PGT machine. Figure 1 (b) illustrates the symbol used to represent the main subsystems —PGT— depicted in Figure 1(a).

Figure 1(a) depicts an expansion-contraction heat scheduling scheme equipped with two reservoirs for heating and cooling, which operate in an alternating and intermittent sequence. Figure 1(b) presents a symbolic scheme representing each power unit within the self-powered power plant.

The PGT prototype shown in Figure 1(a) consists of one or more closed-circuit gas turbines designed for installation in power plants, where they are coupled via a common shaft to all rotating machines in the system. Each PGT operates intermittently based on barothermal pulses. These pulses are generated within dedicated reservoirs and are of two types:

Positive barothermal pulses involve a pressure increase above an equilibrium (reference) pressure, associated with the temperature rise from isochoric heating.

Negative barothermal pulses involve a pressure decrease below the equilibrium pressure, associated with the temperature drop from isochoric cooling.

These pulses are applied to the gas turbine from high-pressure and low-pressure reservoirs, respectively, driving its operation.

To facilitate a clear and concise description of the operating modes of a PGT-based PU with a sVsVs-type thermal cycle, refer to Fig. 2.

Figures 2(a) and 2(b) depict the following processes for the first pair of reservoirs:

Open-Isochoric heat addition in reservoir A.

Open-Isochoric heat extraction in reservoir B.

Figures 2(c) and 2(d) show the corresponding processes for the second pair:

Open-Isochoric heat addition in reservoir C.

Open-Isochoric heat extraction in reservoir D.

The pressure-volume (p - V) diagrams for the sVsVs cycles executed sequentially in reservoir pairs A-B and C-D are presented in Figures 2(e) and 2(f). Each complete operating cycle of the PU consists of these two sVsVs cycles.

Figures 2(g) and 2(h) show pressure-time diagrams for both reservoir pairs. They illustrate the net pressure, defined as the difference between the pressures in reservoirs A and B for the first sVsVs cycle, and between reservoirs C and D for the second.

The concatenation of these sVsVs cycles is illustrated in Figure 3, which plots the resulting pressure pulses over time for one full PGT cycle (comprising two sVsVs thermal cycles).

The configuration requires at least two reservoirs to accumulate thermally active fluid (TWF) for two key reasons:

High-Pressure/Temperature Pulses (Positive pressure pulses):

Reservoirs at the heat source accumulate heated TWF at constant volume, enabling the intermittent generation of high-pressure, high-temperature (barothermal) pulses at the gas turbine inlet.

Low-Pressure/Temperature Pulses (negative pressure pulses):

Reservoirs at the heat sink accumulate cooled TWF at constant volume, enabling the intermittent generation of low-pressure, low-temperature pulses. These create synchronized negative pressure pulses in the gas turbine's evacuation zone.

In one viable design, each high-pressure barothermal pulse applied at the turbine inlet is synchronized with a corresponding negative pressure pulse applied in the evacuation zone.

Finally, Figures 2(b) and 2(d) illustrate the sVsVs cycle on temperature-entropy (T - s) diagrams, highlighting the active heating and cooling phases. These processes are also summarized in Table 2. The cycle consists of two

sequential heat transfer processes: isochoric heat addition (which increases temperature and pressure, producing expansion work) and isochoric heat extraction (which decreases temperature and pressure, producing contraction work). A detailed cycle analysis will be provided in the next section.

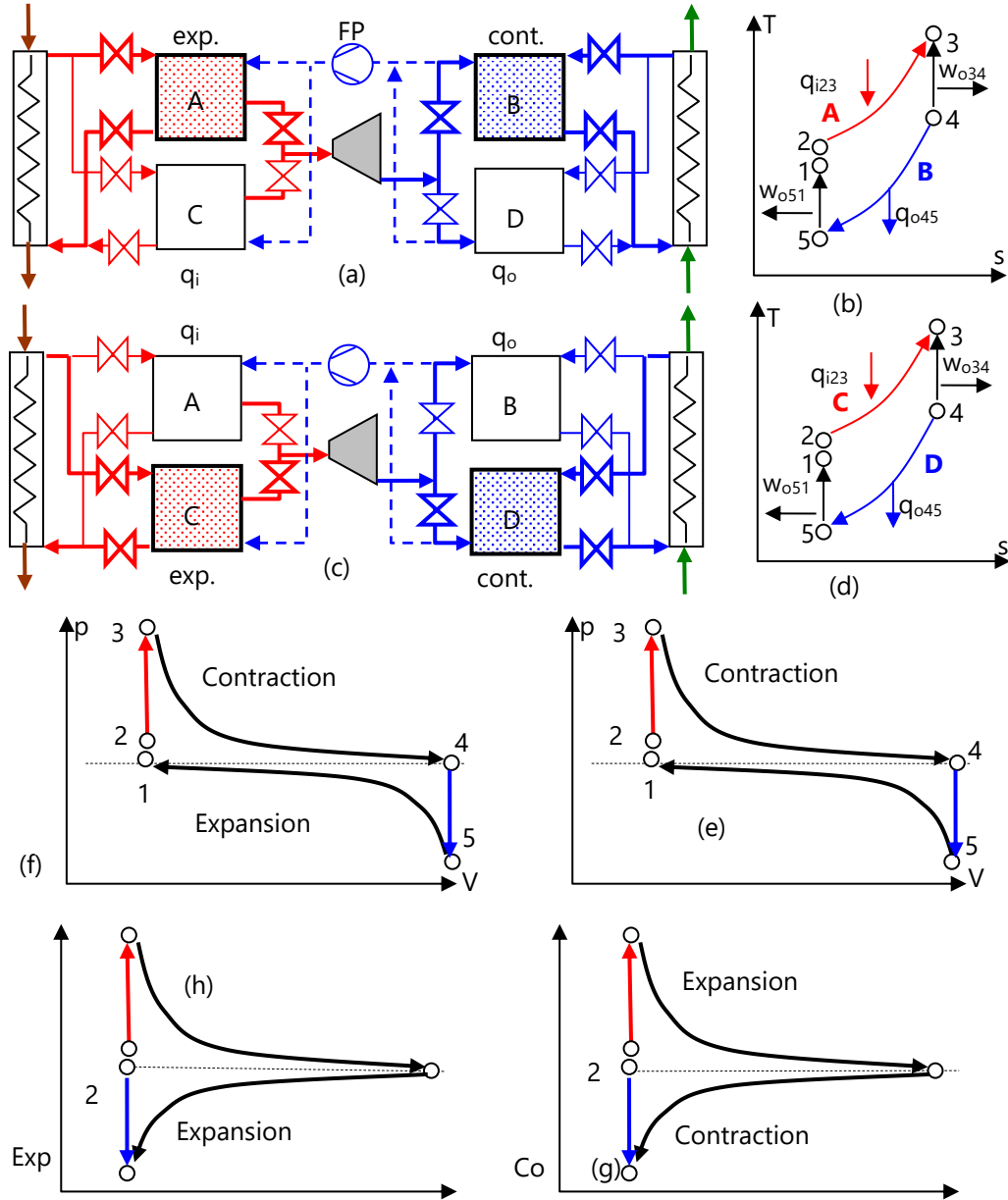


Figure 2: Illustration of the operating procedure through a sVsVs cycle

A complementary process occurs on the low-pressure side. After a reservoir is cooled and contracts, it is connected to the turbine's evacuation zone. This connection increases its pressure from the minimum cooling pressure back to the intermediate reference level. It is then isolated, allowing the next cooled reservoir to take its place. Consequently, when one reservoir is in this intake/compression state, its counterpart is in the isochoric cooling phase. This operating behavior is depicted in Fig. 3, where expansion and contraction pressure are depicted simultaneously giving rise to a greater difference of pressure between positive and negative pressure.

Simultaneously applying positive and negative pressure pulses to the high and low-pressure zones of the barothermal-pulse gas turbine creates a significant pressure differential between its inlet and outlet. This generates a very high initial torque at the start of each barothermal pulse, which attenuates as the Thermodynamic Working Fluid (TWF) expands within the turbine.

In an alternative design, a negative pressure pulse is not applied to the evacuation zone during the heat extraction phase. Instead, heat is rejected to the sink at the reference pressure and temperature. When only positive pressure pulses are applied at the inlet, the achieved pressure differential is only that between the inlet and the equilibrium pressure of the heat sink. Consequently, the torque produced per pulse is lower than in the dual-pulse (positive/negative) configuration.

Within each high-pressure reservoir, the TWF is held at high temperature and pressure. When released in a pulse, it expands adiabatically through the turbine. Notably, this adiabatic expansion approximates a quasi-isothermal process because:

The heat accumulated in the metal of each isochoric heating reservoir and its associated heat exchanger transfers heat to the TWF during expansion.

Conversely, each isochoric cooling reservoir and its cooler transfers heat *from* the heat-extraction fluid during expansion. This process generates useful mechanical work, which can then be converted into electrical energy.

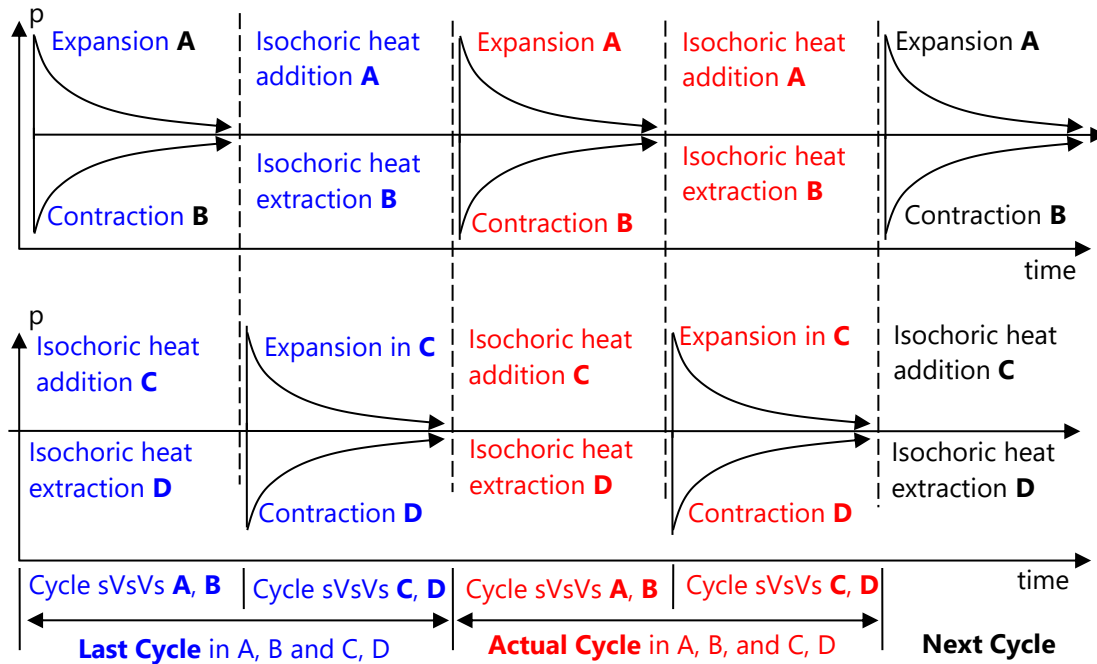


Figure 3: Pressure-time diagrams of the thermal cycle sVsVs and cycle timing synchronization

Table 2 sVsVs thermal cycle execution sequence according to equations (6)-(12) and T-s and p-V diagrams of Fig. 4.

sp	Process task	Sequential sVsVs cycle processes	Thermal-model
1-2	Feed pump (FP). work in	Open adiabatic-isentropic	$w_{i12} = \Delta h_{12}$
2-3	Heating the TWF	Open isochoric heat addition	$q_{i23} = \Delta h_{23}$
3-4	Expansion work out	Open adiabatic-isentropic expansion	$w_{oexp34} = \Delta h_{34}$
4-5	Cooling the TWF	Open isochoric heat extraction	$q_{o45} = \Delta h_{45}$
5-1	Contraction work out	Open adiabatic-isentropic contraction	$w_{ocont51} = \Delta h_{51}$

In Table 2 it is depicted the thermal model corresponding to each cycle process of the sVsVs cycle, highlighting the active heating and cooling phases by means of a sVsVs thermal cycle execution sequence described by equations (6)-(12) and T-s and p-V diagrams of Fig. 4. The analysis of the T-s diagrams depicted in the Fig. 2 (b) and (d) gives rise to the thermal models depicted in Table 2.

2.2 Operating Procedure

The system operates using alternating thermal reservoirs. Generally, when a high-pressure thermal fluid reservoir—pressurized by constant-volume (isochoric) heating—is connected to the gas turbine, the working fluid expands. The pressure-time diagrams of the thermal cycle sVsVs and cycle timing synchronization are depicted in Fig. 3.

According to Fig. 3, this expansion drives the turbine and decreases the fluid's pressure to an intermediate reference level. At this point, the reservoir is isolated from the turbine. A second, pre-heated reservoir then comes into operation, ensuring a continuous power output. Thus, while one reservoir is in the expansion phase, others are simultaneously undergoing pen isochoric heating.

2.2.1 Key Advantages over Conventional Cycles:

The proposed Pulsed Gas Turbine (PGT) technology offers several distinct advantages:

- 1 **No Phase Change:** The Thermal Working Fluid (TWF)—such as helium, dry nitrogen, or dry air—remains in a single gaseous phase. This eliminates the latent heats of vaporization and condensation, simplifying system design.
- 2 **Open -Isochoric Heat Transfer:** Heat addition and rejection occur at constant volume within dedicated, alternately operated reservoirs. This is achieved via forced convection heat transfer.
- 3 **Reduced Cooling Demands:** Turbine blade cooling is not required for operating temperatures below approximately 1200 K.
- 4 **Cascaded Waste Heat Recovery:** Multiple PGT units can be mechanically coupled on a single shaft in a cascade structure, sequenced according to the Heat Transfer Fluid (HTF) temperature gradient. This creates an effective waste heat recovery system because:
 - a It efficiently recovers and utilizes low-grade heat exhaust from upstream turbine stages.
 - b The thermal efficiency of a PGT cycle is not governed by Carnot constraints. Unlike Carnot cycles, PGT efficiency is higher for smaller temperature ranges, which correspond to high temperature ratios. This characteristic significantly enhances the residual heat utilization factor.

Given that the individual efficiency of each PGT unit is substantially higher than that of conventional Rankine-based turbines, and coupled with a superior heat utilization factor, the overall system efficiency is markedly increased. However, even so, self-sufficient capabilities require the addition of another strategy that deals largely with cascaded heat recovery. This strategy, capable of providing self-sufficiency, consists of choosing constant temperature jumps or temperature difference (T_D) between each power unit and short enough to contribute to increasing the self-sufficiency index at the cost of increasing the number of power units.

2.3 PGT-based sVsVs Cycle

Let us begin by clarifying the acronym for the thermal cycle under study: the sVsVs cycle, implemented in a Pulse-based Gas Turbine (PGT) system. The letters in the acronym denote the thermodynamic transformations between successive state points. Here, "s" represents an open isentropic (constant entropy) process, and "V" represents an open-isochoric (constant specific volume) process. Thus, sVsVs describes a sequence of five processes: isentropic, open-isochoric, isentropic, open-isochoric, and isentropic.

Processes of the sVsVs Cycle:

The cycle, illustrated in Table 2, and Fig. 4 consists of the following transformations between state points:

Process 1–2: Open isentropic compression. TWF is transferred from the cold TWF reservoir to the hot TWF reservoir. During this process, the suction and discharge pressures of the compressor or feed pump are almost equal since they only differ in the effect of the load that the mass transfer of the TWF from the cold reservoir to the corresponding hot reservoir entails.

Process 2–3: Closed isochoric heat addition. Heat addition is carried out by means of TWF closed process recirculation under forced heat transfer. The mathematical model of this process is considered the same as if it were an open process due to the flow work required for forced convection heat transfer.

Process 3–4: Open adiabatic-isentropic expansion. Mechanical work is performed by hot TWF open process expansion. The useful mechanical work done by the expansion of the TWF in an open process is due exclusively to the prior addition of heat from a hotter source.

Process 4–5: Closed isochoric heat extraction (no heat rejection). Heat extraction (cooling) is carried out by means of TWF closed process recirculation under forced heat transfer. The mathematical model of this process is considered the same as if it were an open process due to the flow work required for forced convection heat transfer

Process 5–1: Open adiabatic-isentropic contraction. Mechanical work is performed by cold TWF open process contraction. The useful mechanical work done by the contraction of the TWF in an open process is due exclusively to the prior extraction of heat to a cooler heat sink.

These processes are described in detail below:

Process 1–2:

This corresponds to an open, adiabatic, and isentropic compression process driven by a feed pump or gas compressor. It is classified as an "open" process because it involves mass transfer. The work input to the compressor for this adiabatic-isentropic process is given by:

$$w_{i12} = w_{iFP} = \Delta h_{12} = h_2 - h_1 = Cp \cdot (T_2 - T_1) \quad (1)$$

Process 2-3:

Correspond to a open-isochoric heat addition process in which the working fluid is heated.

$$q_{i23} = \Delta h_{23} = h_3 - h_2 = Cp \cdot (T_3 - T_2) \quad (2)$$

Process 3-4:

Correspond to an open adiabatic expansion process in the PGT which undergoes mass transfer while volume increases. Thus the thermal energy in the form of enthalpy is converted into mechanical work, provided that the PGT rotates freely doing expansion work.

$$w_{o34} = w_{oexp34} = h_3 - h_4 = \Delta h_{34} = Cp \cdot (T_3 - T_4) \quad (3)$$

Process 4-5:

Correspond to a open-isochoric heat addition process in which the working fluid is heated without work done because of the constant volume process

$$q_{o45} = \Delta h_{45} = h_4 - h_5 = Cp \cdot (T_4 - T_5) \quad (4)$$

Process 5-1:

Correspond to open adiabatic contraction-based compression process. Thus the thermal energy in the form of enthalpy is converted into mechanical work by contraction (TWF volume decreases in the cold PGT reservoir), provided that the PGT can move freely to permit the contraction-based compression work.

$$|w_{o51}| = |w_{ocont51}| = |h_5 - h_1| = Cp \cdot |T_5 - T_1| = Cp(T_1 - T_5) \quad (5)$$

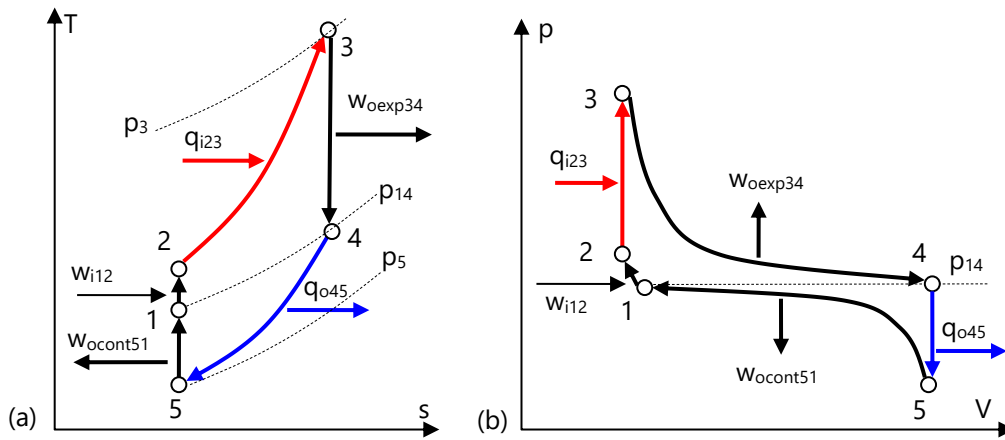


Figure 4: Single PGT-sVsVs hybrid (closed & open processes) thermal cycle. (a): T-s diagram. (b): p-V diagram

The sVsVs thermal cycle is hybrid due to be composed by closed and open processes. While heat transfer is carried out by adding and extracting heat by means of isochoric closed processes, the rest of processes involving work undergo mass transfer. Consequently, the open process-based heat-work interactions are modeled by using enthalpies.

2.4 sVsVs analysis

The analysis of the 4CP VsVs is based on the first law, so that the energy transfer flows include the following energy balances derived from the previous section:

Input heat:

heat added at closed isochoric heat transfer process

$$q_{i23} = \Delta h_{32} = Cp \cdot (T_3 - T_2) \tag{6}$$

Output heat

heat extracted at closed isochoric heat transfer process

$$q_{o45} = \Delta h_{45} = Cp \cdot (T_4 - T_5) \tag{7}$$

Input work

The input work in the sVsVs cycle is due to the pumping effort of the feed compressor. In order to simplify the analysis without loss of generality, the amount of work done on the feed compressor to transfer the working fluid from the cold reservoirs to the hot reservoirs is

$$w_{i12} = \Delta h_{21} = h_2 - h_1 = Cp \cdot (T_2 - T_1) \tag{8}$$

Output work

The work done by expansion along the process 2-3 due to the isochoric heat added is

$$w_{o34} = w_{oexp34} = \Delta h_{34} = Cp \cdot (T_3 - T_4) \tag{9}$$

The work done by contraction along the process 5-1 due to the isochoric heat extracted is

$$w_{o51} = w_{ocont51} = \Delta h_{51} = Cp \cdot (T_1 - T_5) \tag{10}$$

Net useful work

$$w_n = w_{o_{exp34}} + |w_{o_{cont51}}| - \Delta h_{12} = \Delta h_{34} + \Delta h_{51} - \Delta h_{12} \quad (11)$$

Therefore, the thermal efficiency is given by the ratio of the mechanical work to the input heat, yielding

$$\eta_{th} = \frac{w_n}{q_i} = \frac{w_{o_{34}} + |w_{o_{51}}| - \Delta h_{12}}{\Delta h_{32}} = \frac{\Delta h_{34} + \Delta h_{51} - \Delta h_{12}}{Cp \cdot (T_2 - T_1)} = \quad (12)$$

Relevant comments on the framework for addressing Second Law concerns

Below is a discussion regarding to explicitly incorporating an entropy balance consistent with the Second Law, including the global inequality $\Delta s_{sys} + \Delta s_{surr} \geq 0$

The significance of this groundbreaking achievement becomes clear when analyzed using an explicit Second Law entropy balance. During the contraction phase, useful mechanical work is produced without the need for an external input of thermal energy. Instead, the process is accompanied by a controlled heat extraction associated with cooling. Importantly, this heat is not irreversibly dissipated into the environment but is recovered and retained within the system boundaries for later reuse. As a result, the process does not violate the Second Law, since entropy is neither destroyed nor reduced; rather, it is redistributed and managed internally.

For each processing unit (PU), the entropy balance can be expressed as $\Delta s_{(PU)} = \int \delta q_{rec} \cdot T + S_{gen}$ where δq_{rec} denotes the recoverable heat extracted during cooling, and $S_{gen} \geq 0$ is the entropy generated by unavoidable irreversibilities. When the PU is considered in isolation, entropy production is strictly non-negative, fully consistent with the Second Law. However, by reinjection the recovered heat into downstream or upstream processes within the same architecture, the associated entropy flux remains internal rather than being dispersed into the surroundings.

At the system level, the global entropy balance becomes $\Delta s_{sys} + \Delta s_{surr} \geq 0$

In the proposed configuration, Δs_{sys} accounts for the cumulative entropy changes across all cascaded PUs, while Δs_{surr} is minimized by reducing net heat rejection to the environment. Because the majority of the heat associated with cooling is recovered and reutilized internally, the entropy increase of the surroundings is substantially lower than in conventional thermal architectures. The inequality remains satisfied at all times, but the entropy production is spatially confined and functionally exploited rather than lost.

The effective gain in thermal efficiency therefore arises from improved exergy utilization, not from any spontaneous conversion of heat into work without compensation. Mechanical work production is always accompanied by corresponding entropy generation, yet the strategic internal circulation of recovered heat allows the system to operate closer to reversible limits. In practical terms, this translates into a higher fraction of the internally available energy being converted into useful work, while irreversible entropy export is deferred or reduced.

In summary, the cascade arrangement of processing units performing coordinated expansion and contraction processes—combined with systematic recovery, regeneration, and reinjection of cooling heat—constitutes a thermodynamically consistent pathway toward energy self-sufficiency. The Second Law is fully respected: the total entropy of the combined system and surroundings does not decrease. Self-sustaining operation emerges as a consequence of entropy management and internal heat reuse, rather than as an exception to fundamental thermodynamic constraints.

Kelvin–Planck and Clausius compliance disclaimer

The Kelvin-Planck statement of the second law of thermodynamics asserts that *“it is impossible to create a cyclic engine that converts 100% of heat from a single reservoir into net work”*.

The Clausius statement of the second law of thermodynamics asserts that *“it is impossible to construct a device operating in a cycle that transfers heat from a colder body to a hotter body without external work input”*.

On the basis of the statements of Kelvin-Planck and Clausius, the fact of achieving a heat engine enabled to operate without an external energy source on a cycle does not violate the second law in the statements of Kelvin Planck or in that of Clausius.

It is emphasized that, while the proposed architecture conforms to either the Kelvin-Planck or Clausius statements of the Second Law of Thermodynamics, the condition of self-sufficiency does not require an external heat source. According to the statements of Kelvin-Planck and Clausius, **there is no reference to the prevailing need for an external heat source**. This means that the existence of self-sufficient machines does not necessarily have to violate the second law of thermodynamics.

In particular, the system does not operate by extracting heat from a single thermal reservoir and converting it entirely into work, nor does it induce net heat transfer from a colder body to a hotter one without external compensation. All work-producing stages are accompanied by corresponding entropy generation and compensating heat flows, and at no point is mechanical work obtained from heat alone without an associated entropy increase. Heat recovery and reinjection occur exclusively within the system boundaries and serve to reduce irreversible external heat rejection, not to abolish it. Consequently, the apparent performance gains arise from internal heat reutilization, exergy preservation, and entropy flow management across multiple interacting control volumes, rather than from any prohibited thermodynamic process. When evaluated as a closed system interacting with its surroundings, the overall operation remains fully compliant with both Kelvin-Planck and Clausius formulations of the Second Law.

2.5 How to achieve a high amount of contraction work with respect to expansion work

In order to achieve a similar structure in dimensional terms between the PGT-based rotary actuators endowed with the ability to convert heat to work with the same actuator volume at the cost of different temperatures and pressures, a constant temperature jump or drop per temperature (T_D) is used between each of the PUs that make up the PU cascade.

Each Power Unit (PU) completes one PGT cycle by executing two sequential sVsVs thermal cycles. These cycles operate in a complementary manner: while one sVsVs cycle performs mechanical work through expansion and contraction, the other simultaneously undergoes heat addition and extraction.

To proceed with the study of the SSPM, it is essential to characterize each PU based on the properties of its thermal cycle. This analysis focuses on the behavior of the PGT-sVsVs cycle with respect to the isochoric temperature drop T_D , defined as $T_D = T_3 - T_1$. The goal is to identify a constant temperature drop that ensure acceptable performance for the complete SSPM which involves each PU within an operating range suitable for cascade integration downstream in the SSPM.

The ratio RW of the mechanical work done by contraction to expansion of the TWF is expressed as:

$$WR = \frac{W_{ocont}}{W_{oexp}} \quad (13)$$

So, to clarify this concept, for each PU, the ratio RW depends on T_D such that when T_D tends to zero, WR tends to one. The ratio of contraction to expansion work cannot be equal to one. If the temperature drop between each cascaded PU approaches zero, the ratio WR tends to one. In this limit, $T_1 = T_3$, meaning no heat transfer occurs, and consequently no power can be developed. As T_3 approaches T_1 , the amount of useful work obtained from cooling increases, which enhances thermal efficiency. However, achieving this requires increasing the number of PUs. Consequently, it is necessary to determine an optimal temperature jump that maximizes net profit by balancing improved efficiency against the higher cost associated with adding more PUs.

2.6 Integration of the PGT sVsVs cycle into a cascade of PUs to implement a SSPM [15]

A systematic methodology to implement a cascaded group of PUs operating with a constant temperature difference T_D is proposed: The cases studies comprehend four T_D values applied on the study of 4 SSPMs-based case studies operating by means of thermal cycles of the type PGT-sVsVs, where top temperature T_3 is fixed in 1000 K for the first PU of each cascaded SSPM cascade and the corresponding temperature T_1 according the chosen T_D . By processing the data of Table 2 according to the thermodynamic model of the proposed thermal cycle described along equations (1-6 and 7-12), a useful set of data is obtained as results of the analysis, as function of the constant T_D for each case which is depicted in Table 3. The mentioned results include the high and low temperatures, the specific flows of input heat and output heat, as well as useful mechanical work, and with the aim of comparison purposes the thermal efficiency and Carnot factor is also depicted.

The cascaded PUs-based structure is configured according to the Fig. 2(a) and 2(c). Observing Fig. 5 it can be noted that while the heat supply system includes a set of cascaded heat exchangers to supply heat to all cascaded PUs of the SSPM, the cooling heat from the reservoirs responsible for the vacuum is extracted from them in a cascade and recovered to be fed back into the internal heat supply system. The unique circuit responsible for the circulation of the HTF enabled to add and extract heat to/from the hot and cold reservoirs is essential to achieving self-sustainability capabilities.

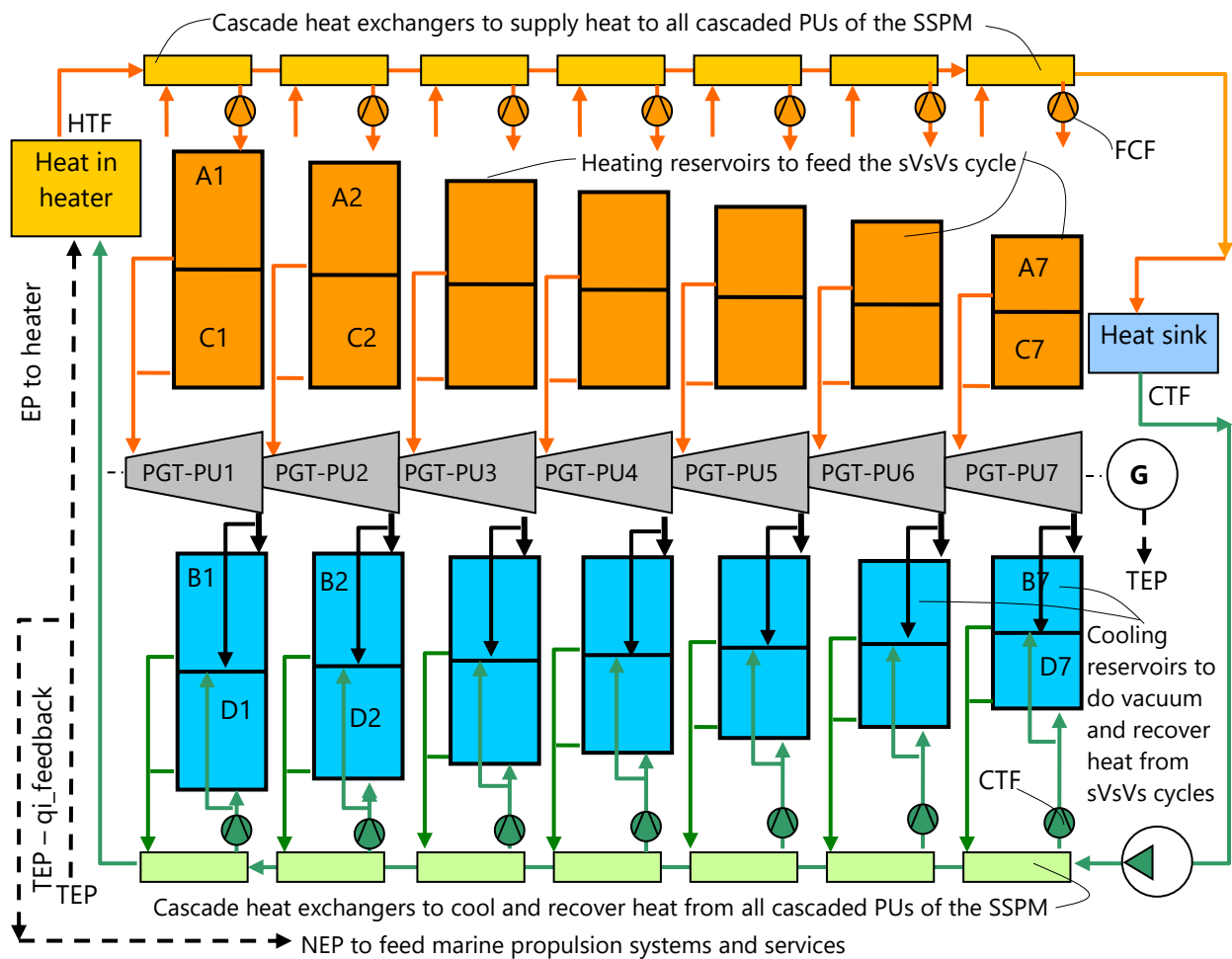


Figure 5: Structure of a SSPM composed of seven cascaded PGT-based PUs, showing some of the most significant components: [5], [18], [19]

Fig. 5 illustrates the main components of a SSPM composed of cascaded PUs made of rotary actuators based on PGTs [5], [18], [19]. Among the main parts, each PU shows:

- Two TWF's reservoirs for heat addition

- Heat addition piping responsible for raising the TWF pressure and temperature by means of the HTF circulation
- TWF recirculation ducts via a recirculation compressor for heat addition to the TWF by forced convection
- A gas turbine-based rotary actuator that operates using pressure and temperature pulses (PGT)
- Two TWF reservoirs for heat extraction cooling
- HTF extraction circuit piping or ducts from the reservoirs responsible for generating a vacuum
- TWF recirculation circuit piping or ducts via a recirculating compressor for heat extraction from the TWF by forced convection
- Recirculation pump for HTF (thermal oil or equivalent)
- Recirculation rotary feed compressors to activate forced convection heat transfer to/from the HTF (thermal oil) to/from the TWF of any PU of the SSPM.
- Feed Pump for each PU —not represented in the figure

With regard to the structure depicted in Fig. 5 it is worth noting that the volume of the TWF tanks, both hot and cold, for each power unit (PU) is different; however, the volume of each PGT-based rotary actuator for each PU is identical. This design strategy allows for a significant reduction in the manufacturing and maintenance costs of the rotating machines, as they are identical because they only have to withstand relatively small temperature and pressure changes, which implies minimal thermal variations under steady-state operating conditions.

Therefore, the next section on design addresses the proposed case studies that take into account the aforementioned observation.

Since the ship power technology based on SSPMs must replace conventional propulsion systems including fossil fuels-based combustion engines and nuclear power, which will be the power source for ship propulsion systems, we will call such self-sustaining power systems "self-sustaining power generators" (SSPG).

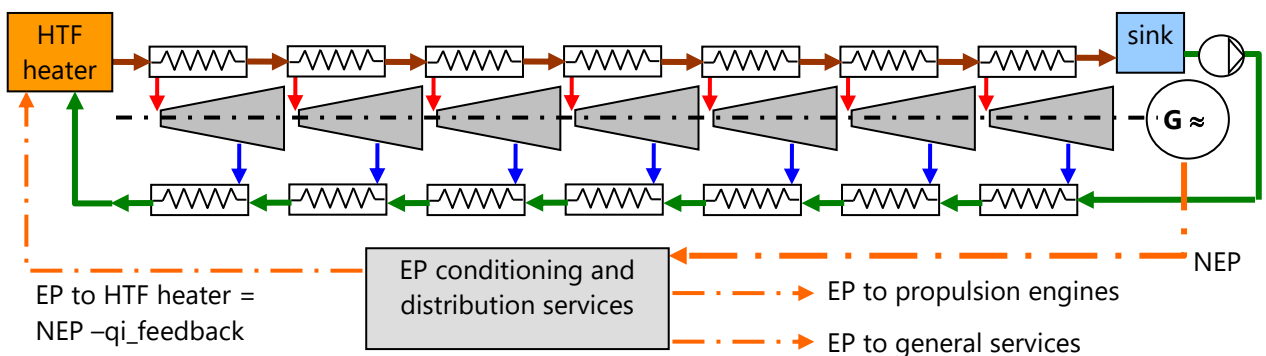


Figure 6: Symbolic illustration of an SSPM structure composed of seven cascaded PGT-based processing units (PUs), showing a schematic of electrical power scheduling. [5], [18], [19]

Comparing the contents of figures 5 and 6, it is observed that the energy distribution strategy is adapted to drive a generic ship propulsion system. The aforementioned strategy indicates that any SSPM that satisfies an energy demand is susceptible to adaptation to any industrial application that is not limited by the excess volume or weight of the plant.

2.7 Case studies on a SSPM

In the proposed case study, an SSPM composed of 7 PGT-based PUs conditioned by the sVsVs cycle is considered. Using equations 6 to 13, the information shown in Table 3 is obtained. In this table, computation data and results for helium as working fluid is depicted. Along the analysis real TWF data used belongs to the

database provided by Lemmon E. W., et all, (2007), [13]. In Table 4 main results from cycle data is depicted. For the studied case a top temperature of 1000 (K) is chosen, while the temperature difference or drop T_D is assumed as 100 K between each cascaded PU. This means that every SSPM is completed by means of 7 PGT-based PUs. Considering helium as TWF, thermal and mechanical losses are grouped as losses factor (LF) = 0.9 which is interpreted as a thermal efficiency of 90 (%), while isentropic efficiency or losses (L_{eff}) are assumed as 0.9 which contributes to an efficiency of 90 (%).

2.7.1 SSPM composed by 7 PUs each driven by a PGT-sVsVs cycle using helium and T_D : 100 K

The number of PUs in each SSPM is associated with the operating temperature range ($T_H-T_L = 1000-300K$) and the temperature drop T_D between each cascaded PU, such that if an operating temperature range between 1000 and 300 (K) is chosen, the number of possible 100 K jumps is the ratio between range and temperature jump; that is $(1000-300)/100 = 7$ PUs. Therefore Table 3 depicts the results for each PU.

Table 3: Processed data for a SSPM composed by 7 cascaded PGT-based PUs into the temperature range of 1000-300 K.

sp	T(K)	p(bar)	$v(m^3/kg)$	$u(kJ/kg)$	$h(kJ/kg)$	$s(kJ/kg. K)$
PU 1; TD = 100 K						
1	900.00	20.00	0.9372	2810.40	4684.90	27.491
2	908.94	20.50	0.9235	2995.80	4736.57	27.491
3	1000.00	22.55	0.9235	3122.20	5204.80	27.789
4	953.17	20.00	0.9924	2976.10	4985.38	27.789
5	866.00	18.17	0.9924	2704.40	4507.80	27.491
PU 2; TD = 100 K						
1	800.00	20.00	0.8334	2498.80	4165.70	26.879
2	807.87	20.50	0.8211	2523.40	4211.26	26.879
3	900.00	22.84	0.8211	2810.60	4685.70	27.216
4	853.58	20.00	0.8890	2665.80	4468.08	27.216
5	766.00	17.95	0.8890	2392.80	3988.50	26.879
PU 3; TD = 100 K						
1	700.00	20.00	0.7296	2187.20	3646.50	26.186
2	908.94	20.50	0.7189	2208.80	3686.61	26.186
3	800.00	23.20	0.7189	2499.00	4166.60	26.572
4	754.01	20.00	0.7857	2355.50	3950.87	26.572
5	666.20	17.67	0.7857	2081.80	3470.30	26.186
PU 4; TD = 100 K						
1	600.00	20.00	0.6258	1875.60	3127.30	25.386
2	908.94	20.50	0.6167	1894.20	3161.97	25.386
3	700.00	23.68	0.6167	2187.40	3647.60	25.836
4	654.35	20.00	0.6823	2045.00	3433.31	25.836
5	566.30	17.31	0.6823	1770.40	2951.40	25.386
PU 5; TD = 100 K						
1	500.00	20.00	0.5221	1563.90	2608.10	24.439
2	504.94	20.50	0.5144	1579.40	2636.77	24.439

3	600.00	24.36	0.5144	1875.80	3128.60	24.977
4	554.57	20.00	0.5787	1734.00	2915.12	24.977
5	466.70	16.83	0.5787	1460.00	2434.10	24.439
PU 6; TD = 100 K						
1	400.00	20.00	0.4183	1252.20	2088.80	23.281
2	404.00	20.50	0.4122	1264.70	2112.13	23.281
3	500.00	25.37	0.4122	1564.20	2609.80	23.946
4	454.70	20.00	0.4751	1422.70	2396.50	23.946
5	367.40	16.16	0.4751	1150.50	1918.30	23.281
PU 7; TD = 100 K						
1	300.00	20.00	0.314540	940.44	1569.50	21.787
2	303.00	20.50	0.309980	949.82	1587.06	21.787
3	400.00	27.05	0.309980	1252.50	2091.10	22.654
4	354.54	20.00	0.3711	1110.50	1876.63	22.654
5	268.50	15.15	0.3711	842.06	1404.30	21.787

2.7.2 Main results of a SSPM of 7 PGT-based PUs derived from data in Table 3.

Table 4 illustrates the main results of the SSPM of 7 PGT-based PUs, including the most relevant data from the studied SSPM. Therefore, to facilitate understanding of the results in Table 4, the meanings of the relevant SSPM parameters are illustrated in the following list:

Table 4: Results the cascaded PUs from data processed in Table 3

PU	1	2	3	4	5	6	7	Total
LF(%)	0.90	0.90	0.90	0.90	0.90	0.90	0.90	0.90
Is_eff(%)	0.90	0.90	0.90	0.90	0.90	0.90	0.90	0.90
T _{3_sVsVs}	1000.00	900.00	800.00	700.00	600.00	500.00	400.00	
T _{1_sVsVs}	900.00	800.00	700.00	600.00	500.00	404.00	300.00	
qi_top/PU(kJ/kg)	468.23	474.44	479.99	485.63	491.83	497.67	504.04	3401.84
q _{o45} (kJ/kg)	477.58	479.58	480.57	481.91	481.02	478.20	472.33	3351.19
q_rec(kJ/kg)	477.58	479.58	480.57	481.91	481.02	478.20	472.33	3351.19
mean_rec_T(K)	926.59	826.79	350.36	627.18	527.29	427.35	327.27	
w _{i12} (kJ/kg)	51.67	45.56	40.11	34.67	28.67	23.33	17.56	241.56
w _{o34} (kJ/kg)	197.48	195.86	194.16	192.86	192.13	191.97	193.02	
W _{o51} (kJ/kg)	159.39	159.48	158.58	158.31	156.60	153.45	148.68	
RW(%)	80.71	81.43	81.68	82.09	81.51	79.93	77.03	
w _n =W _{o34} +W _{o51} -w _{i12} (kJ/kg)	305.20	309.78	312.63	316.50	320.07	322.09	324.15	2210.41
η _{th} /PU	65.18	65.29	65.13	65.17	65.08	64.72	64.31	
V _{reserv} (m ³ /kg)/PU	0.9235	0.8211	0.7189	0.6167	0.5144	0.4122	0.3100	4.32
V _{tot} (m ³ /kg)/PU	0.9924	0.8890	0.7857	0.6823	0.5787	0.4751	0.3711	4.77
ΔV_actb(m ³)	0.0689	0.0679	0.0668	0.0656	0.0643	0.0628	0.0612	0.4575
p _{ref} (bar)/PU	20.00	20.00	20.00	20.00	20.00	20.00	20.00	
Δp (bar)/(PU-cycle)	2.05	2.34	2.70	3.18	3.86	4.87	6.55	
qi_feedback_PU1=(h ₃ -h ₅) (kJ/kg-cycle)								697.00
Output net work (kJ/kg-cycle)								1513.41

The useful work performed by each PU should ideally be approximately equal across all units of the SSPM. However, when designing a plant to operate with a temperature drop of 100 K between PUs, which is excessively high to maximize self sufficiency and minimize the number of PUs in the SSPM, there is some deviation in the net work out between PUs, also due to the Feed pump work required to feedback the TWF in each PU of the SSPM. This results in excessive differences between the individual work outputs of each PU, as shown in Table 4, and Fig. 7. This results in the fact that the net work output of each PU is different, being relatively high for the first PU, PU1, and considerably lower for the last PO or PU7. This results in the net work output of each unit being different, being relatively normal at approximately 300 kJ/kg for the first unit, PU1, and considerably higher for the last unit, PU7 at approximately 325,000 kJ/kg.

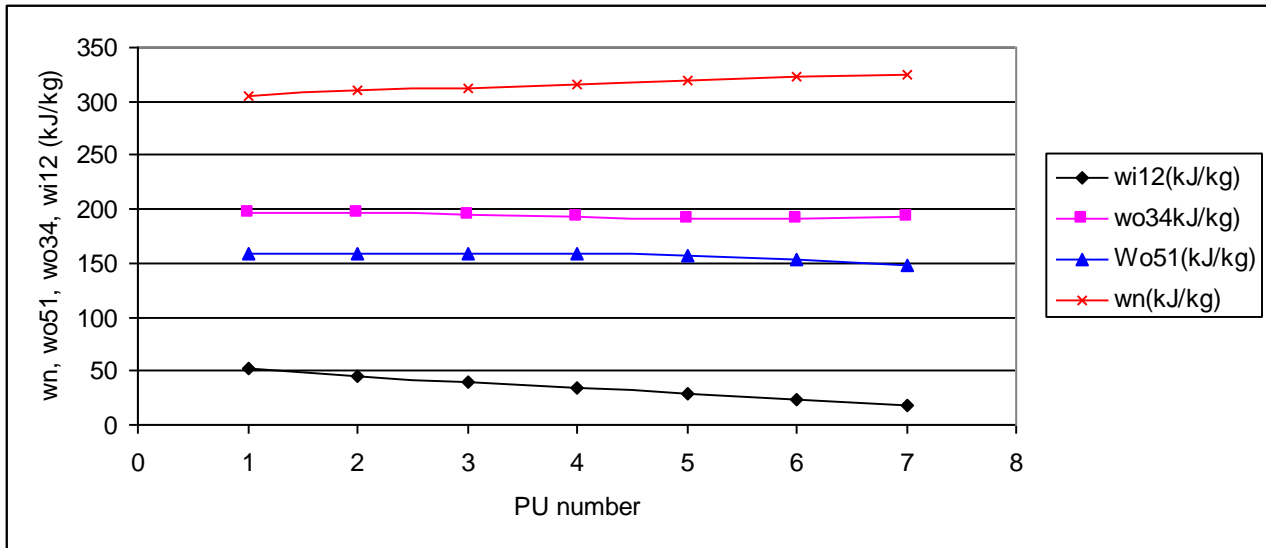


Figure 7: illustration of the input feed pump work, output expansion, output contraction and resultant output net work of the seven cascaded PUs

Given the interdependence between the critical and common parameters inherent in all the PUs of the SSPM case study, which are relevant to the key analyses and conclusions regarding the prototype design, the following parameters are considered useful for analyzing the results using the data presented in Table 5. Among all the relevant data presented in Table 5, the total useful work per cycle is essential. However, it is also important to determine the total work output delivered by each SSPM, the feedback heat added to the first PU of the cascaded PUs, and the net useful work output as a function of the constant temperature drop (TD) set at 100 K, for a fixed reference pressure chosen to be the same for each PU of the designed SSPM.

Table 5: Concept description of the results derived from processing cycle data from table 4 for a SSPM composed of 7 PGT-based PUs

NPU _s /SSPM: number of PUs/SSPM	7
T _D (K): constant temperature drop between cascaded PUs	100
LF (%): mechanical and thermal losses	0.9
Is _{eff} (%): isentropic efficiency of each actuator (PGT)	0.9
∑qi _{PUi} /SSPM(kJ/kg): total heat inlet to the SSPM PUs	3401.84
∑qo ₄₅ (kJ/kg): total cooling heat output/SSPM	3351.19
∑q _{rec} (kJ/kg): total heat recovered/SSPM= qo ₄₅	3351.19
∑wi ₁₂ (kJ/kg): input feed pump work	241,56
∑Wo ₃₄ (kJ/kg): expansion output useful work/SSPM	1357.48
∑Wo ₅₁ (kJ/kg) contraction output useful work/SSPM	1094.49
RW: average ratio of contraction to expansion work	80.62
∑w/PU (kJ/kg-cycle): ∑Wo ₅₁ +∑Wo ₃₄ -∑wi ₁₂ = net SSPM useful mechanical work/SSPM	2210.41

$\eta_{th}/SSPM$: Average thermal efficiency of PUs/SSPM	64.98
$\sum V_{reserv}(m^3/kg)/PU$: Reservoir volume /SSPM	4.32
$\sum V_{tot}(m^3/kg)/PU$: Total thermal volume of the SSPM; $\sum V_{reserv} + \sum \Delta V_{act}$	4.77
$\sum \Delta V_{act}(m^3) = \sum V_{tot} - \sum V_{reserv}$: actuator volume consisting of PGT-based turbines	0.458
$p_{ref}(\text{bar})/PU$: initial pressure of the sVsVs cycle	20
$q_{i_feedback}(PU1) = h_3 - h_5(\text{kJ/kg-cycle})$ (Amount of heat added to the PU1)	697.00
$\sum w/PU$ (kJ/kg-cycle) — $q_{i_feedback}(PU1)w_n/SSPM =$ output useful work of the SSPM)	1513.41

3 Scaling SSPM dimensions too meet power demand in marine propulsion applications

To meet the energy demands of marine ship applications including submersible vehicles, it is necessary to satisfy the needs of energy support to the following essential services:

- redundant main propulsion power equipment.
- onboard electrical power demand including cargo maintenance and essential services
- onboard thermal power demands
- Autonomous emergency power supply services

By proportionally scaling the volume of the hot and cold PU tanks of the SSPM's TWF to meet the power demand, the approximate plant volume and weight can be estimated.

Ideal power is usually estimated from the specific work (the corresponding input or output work done per unit time) of one kg of TWF per second (s). That is, the product of the mass flow rate ($\dot{m} = \text{mfr}$) of TWF and the specific work w_n .

$$P = \text{Power} = \dot{m} \cdot w [(kg/s) \cdot (kJ/kg)] \rightarrow (kJ/s) \rightarrow kW \quad (14)$$

3.1 Modeling a SSPM-based MPS through PGT-based PUs and the sVsVs Cycle

The objective of the propulsion modeling task is to determine the actual electrical power demand to satisfy two basic needs such as sufficient propulsive thrust and, electrical power to meet the total demand of resource exploitation tasks.

Ideal power is usually estimated from the specific work (the corresponding input or output work done per unit time) of one kg of TWF during a second (s). That is, the product of the mass flow rate ($\dot{m} = \text{mfr}$) of TWF and the specific work. When specific work is expressed by means of an enthalpy change, power is expressed according to previous Eq. (14) as $P = \dot{m} \cdot w$.

As shown in Figs. 8-13, it is depicted the ideal power ideally delivered by an SSPM designed according to specified characteristics.

The real adiabatic expansion and contraction of the TWF along the processes carried out in the SSPM exhibit inherent losses due to irreversibilities. Depending on the design profile and operating conditions, these losses can exceed 20%. However in real situations the input power (P_{in}) according Eq. (16), which means the required power to satisfy a given thrust under ideal conductions, is the ratio of the specific thermodynamic work to the overall propulsion efficiency (η_p). Therefore, the input power is described considering the propulsion efficiency as

$$P_{IN} \approx \frac{P}{\eta_p} = \frac{\dot{m} \cdot w}{\eta_p} \quad (15)$$

However, in this approach, these losses are disregarded, and therefore the ideal case will be assumed.

Core Innovation: The PGT moves away from traditional constant-pressure combustion turbines. It operates intermittently using simultaneous "barothermal pulses"—positive pressure pulses from isochoric (constant volume) heating and negative pressure pulses from isochoric cooling.

Table 6 shows the total thermodynamic volumes of the SSPMs. Thermodynamic volume is important for estimating the volume occupied by each SSPM, but also as data for estimating the weight associated with the reservoirs responsible for a high proportion of the volume of each SSPM. Table 6 illustrates the fundamental data for proceeding with the scaling procedure for the case study.

Table 6: Illustration of the case study for analyzing the power scaling methodology.

NPU	7
Feedback heat (kJ/kg): $q_{i_feedback} (PU1) = h_3 - h_5$ (kJ/kg-cycle)	697
work/cycle (kJ/kg): $\sum w/PU$ (kJ/kg-cycle) – $q_{i_feedback}(PU1)$:	1513.4
Thermal V(m ³)/SSPM:	4.77
T _D (K)/PU	100

The data in Table 7 are interpreted such that, with reference to case studied, for a TWF flow rate of 1 kg/s and a cycle time of 1 second, a thermodynamic volume of 5.4 m³ is required to obtain 1.513 MW of power. Likewise, for a TWF flow rate of 10 kg/s and a cycle time of 1 second, a thermodynamic volume of 54 m³ is required to obtain 15.13 MW of power. Once the total energy demand is known, dimensional scaling is carried out, which estimates, among other data, the total thermodynamic volume, which allows for an approximate estimate of the total mass of SSPM.

Table 7: Dimensional scaling results of SSPM plants according to the case study results.

SSPM cycle (s)	1	2	5	10	15	20
\dot{m} (kg/cycle): 1 ; Total Thermal Vol (SSPM) = $\dot{m} * V_{SSPM}$ (m ³): 4,77						
\dot{m} (kg/s-cycle)	1,00	0,50	0,20	0,10	0,07	0,05
P(MW)	1,51341	0,76	0,30	0,15	0,10	0,08
\dot{m} (kg/s-cycle): 10 ; Total Thermal Vol (SSPM) = $\dot{m} * V_{SSPM}$ (m ³): 47,7						
\dot{m} (kg/s-cycle)	10,00	5,00	2,00	1,00	0,67	0,50
P(MW)	15,1341	7,57	3,03	1,51	1,01	0,76
\dot{m} (kg/s-cycle): 50 ; Total Thermal Vol (SSPM) = $\dot{m} * V_{SSPM}$ (m ³): 238,5						
\dot{m} (kg/s-cycle)	50,00	25,00	10,00	5,00	3,33	2,50
P(MW)	75,6705	37,84	15,13	7,57	5,04	3,78
\dot{m} (kg/s-cycle): 100 ; Total Thermal Vol (SSPM) = $\dot{m} * V_{SSPM}$ (m ³): 477						
\dot{m} (kg/s-cycle)	100,00	50,00	20,00	10,00	6,67	5,00
P(MW)	151,341	75,67	30,27	15,13	10,09	7,57
\dot{m} (kg/s-cycle): 200 ; Total Thermal Vol (SSPM) = $\dot{m} * V_{SSPM}$ (m ³): 954						
\dot{m} (kg/s-cycle)	200,00	100,00	40,00	20,00	13,33	10,00
P(MW)	302,682	151,34	60,54	30,27	20,18	15,13
\dot{m} (kg/s-cycle): 500 ; Total Thermal Vol (SSPM) = $\dot{m} * V_{SSPM}$ (m ³): 2385						
\dot{m} (kg/s-cycle)	500,00	250,00	100,00	50,00	33,33	25,00
P(MW)	756,705	378,35	151,34	75,67	50,45	37,84

3.2 Re-scaling the plant by changing the reference pressure of the cycle sVsVs

The design volume approximately follows a linear function inverse to the pressure (higher pressure means lower volume and vice versa). This thermodynamic property can be used to scale the design of a prototype without significant computational effort.

Table 7 represents also the scaling data for the case of cycle variation. This is useful for the general case of asynchronous engines. Therefore, in Figures 8-13 it is depicted the profile of the power (MW) as a function of mass flow rate (kg/s) and cycle time (s) for a given reference pressure (bar) and V_{tot} (m³).

The volume obtained for a design can be reduced or enlarged simply by modifying the reference pressure. In the case of Table 7, a reference pressure of 20 bar has been used; however, by choosing a reference pressure of 100 bar, the volume would be reduced by 100/20, that is, 5 times less volume for 100 bar than for 20 bar, which provides the opportunity to significantly reduce the total volume of the installation.



Figure 8: Power (MW) as a function of mass flow rate and cycle time for a given reference pressure of 20 bar and v_{tot} (m3) = 4,77

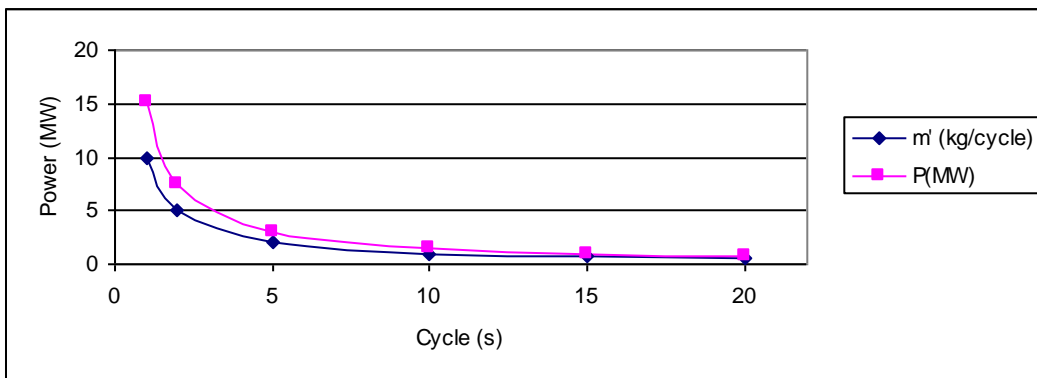


Figure 9: Power (MW) as a function of mass flow rate and cycle time for a given reference pressure of 20 bar and v_{tot} (m3) = 47,7

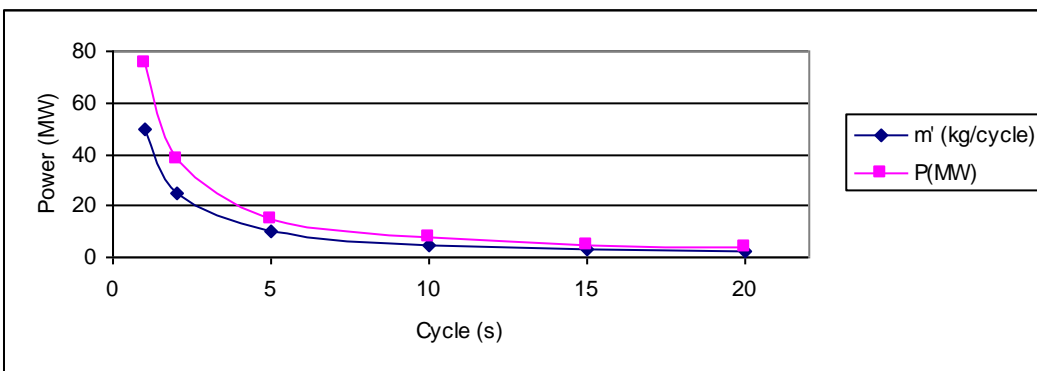


Figure 10: Power (MW) as a function of mass flow rate and cycle time for a given reference pressure of 20 bar and v_{tot} (m3) = 238

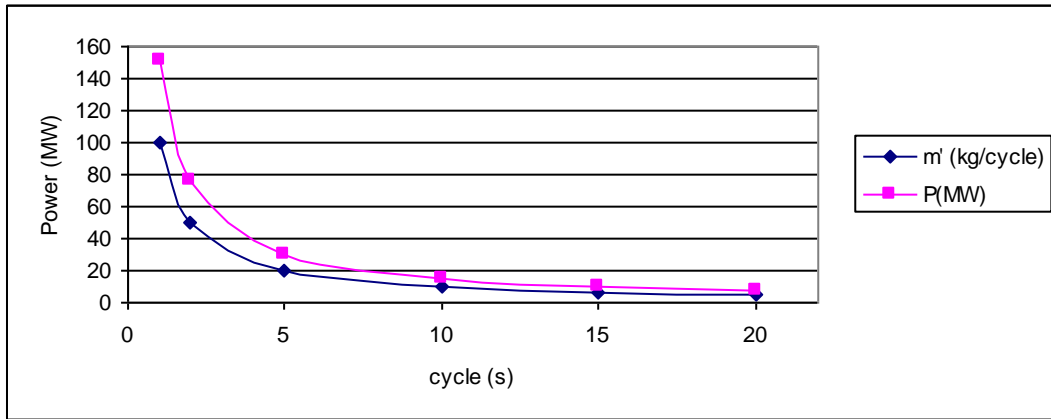


Figure 11: Power (MW) as a function of mass flow rate and cycle time for a given reference pressure of 20 bar and $v_{tot} \text{ (m}^3\text{)} = 477$

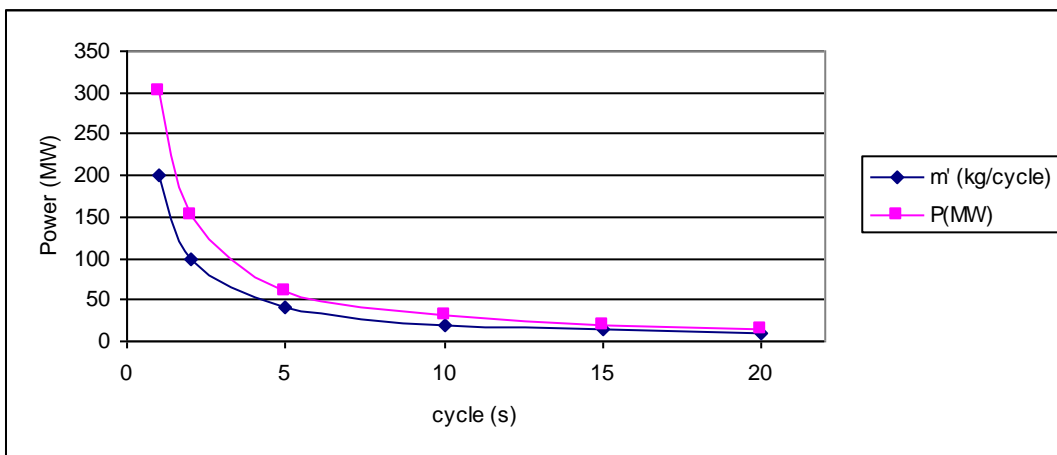


Figure 12: Power (MW) as a function of mass flow rate and cycle time for a given reference pressure of 20 bar and $v_{tot} \text{ (m}^3\text{)} = 954$

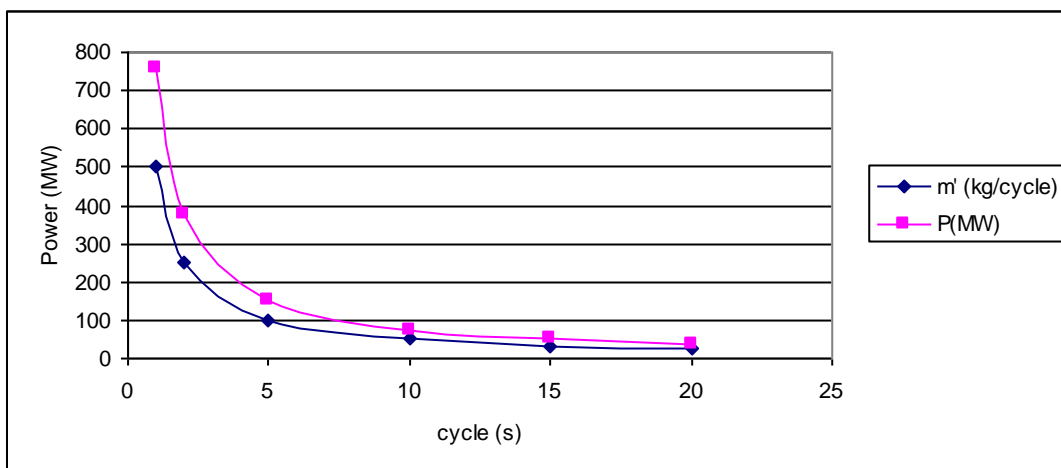


Figure 13: Power (MW) as a function of mass flow rate and cycle time for a given reference pressure of 20 bar and $v_{tot} \text{ (m}^3\text{)} = 2385$

3.3 Electrical Ship Propulsion Architecture

This subsection provides a brief description of the architecture for integrating SSPMs into a ship's propulsion system. This assembly is illustrated in Fig. 14, clarifying the use of electric propulsion in ships, which gained significant importance starting in the 1990s, [21], especially in cruise ships, cargo vessels, fishing vessels, and warships, including submarines. The system shown in Fig. 14 has inherent redundancy by having at least two SSPM units for the supply of electrical power. The generated electrical energy feeds a high-voltage bus, which in turn supplies power to the electric propulsion motors, the SSPM feedback, and the ship's service loads.

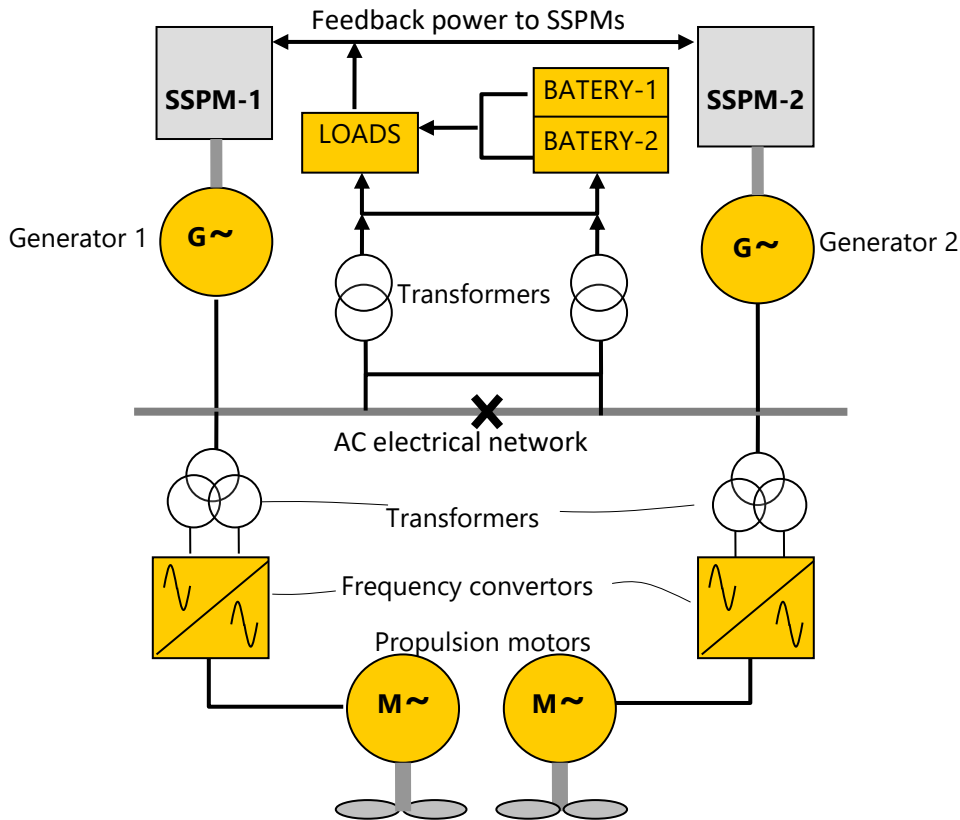


Figure 14: Illustration of a simplified architecture of a self-sustaining energy-assisted marine propulsion system.

The architecture shown in Fig 4 includes simple redundancy in all critical elements: generators, transformers, motors, electrical accumulators and essential services (not shown)

Benefits include:

- 1 Energy Efficiency: Since it does not use fossil or nuclear fuels, the concept of thermal efficiency is irrelevant; rather, the concept of "self-sufficiency index" should be used [22]. The resulting installation is highly efficient because an Energy Management System (PMS) optimizes load distribution to meet total demand according to (the "power plant" concept).
- 2 Emissions: Zero emissions of both CO₂ and NO_x because it does not use combustion engines.
- 3 Reduced Maintenance: Engines based on SSPMs are shared among the propulsion systems and can be shut down when not needed, reducing wear and tear.
- 4 Noise Reduction: It eliminates the mechanical transmission from the engines to the propellers, reducing radiated noise.
- 5 High Availability: The system can be designed to offer high redundancy and reliability. For example, a pair of constantly charged batteries that allow for the startup maneuver of an SSPM unit.

4 Analysis of results

Based on the content of the article, a detailed analysis of the results obtained for the proposed SSPM and its application to marine propulsion is presented. The results analysis is divided into three key areas: the performance of a single Power Unit (PU), the cascaded performance of the complete SSPM, and the scalability of the system for practical marine applications.

4.1. Validation of the Central Thermodynamic Cycle (Power Unit)

The fundamental result is the successful simulation of the sVsVs thermodynamic cycle within a single PGT-based Power Unit. The analysis confirms the principle that useful work can be generated by both expansion (heat addition) and contraction (heat extraction).

4.1.1 Dual Work Production: The data in Table 4 for each Power Unit (PU1 to PU7) show two distinct positive work productions:

w_{034} (kJ/kg): Work by expansion (heating of the TWF).

w_{051} (kJ/kg): Work by contraction (cooling of the TWF).

4.1.2 Ratio between contraction and expansion work (RW): A key performance indicator is the ratio between the contraction and expansion work. The results show that, for a temperature drop (TD) of 100 K between cascaded units, this ratio is exceptionally high, averaging 80.62% across the seven processing units (PUs). This quantitatively demonstrates the central claim of the text: a significant amount of useful work can be obtained from the cooling process, representing a radical departure from conventional cycles that rely solely on expansion.

4.1.3 Thermal efficiency (η_{th}/PU): The thermal efficiency of each PU is calculated to be between 64.3% and 65.3%. This value is exceptionally high and, as stated in the text, appears to defy conventional thermodynamic constraints (such as Carnot efficiency), since the cycle recovers and reuses waste heat from the contraction process. The analysis attributes this to the unique structure of the sVsVs cycle and the cascade heat recovery strategy.

4.2. Integrated System Performance (7-PUs-based SSPM)

The most significant results come from the integration of the seven processing units (PUs) into a complete SSPM, as detailed in Table 5. The data confirm that the cascade structure successfully creates a self-sustaining cycle.

4.2.1 Energy Balance and Self-Sufficiency: The cascade is designed so that the heat dissipated by the cooling process of each subsequent PU (q_{045}) is recovered ($\sum q_{rec}$) and reinjected into the first PU. The analysis shows a total heat recovery of 3351.19 kJ/kg across the entire SSPM. This recovered heat is used to supplement the initial heat input. The key indicator of self-sufficiency is the useful work output of the SSPM, calculated as:

Total net work ($\sum w/UP$) – Heat reinjected into UP1 ($q_{i_feedback}$) = 1513.41 kJ/kg-cycle.

This positive value of 1513.41 kJ/kg-cycle is the main achievement. It demonstrates that the system produces more useful mechanical work than the initial heat required to start the cycle of the first power unit (UP), thus proving its **self-sustaining capacity**.

4.2.2 Cumulative net work: The system produces a total useful net work ($\sum w/UP$) of 2210.41 kJ/kg-cycle. This is the sum of the expansion (1357.48 kJ/kg) and contraction (1094.49 kJ/kg) work in the seven units, minus the work consumed by the feed pumps (241.56 kJ/kg).

4.2.3 Challenge of Uniform Work Distribution: The results in Table 4 and Figure 7 reveal a design nuance. While the objective was to obtain the same work output from each power unit (PU), the data show a variation: the net work of PU7 (324.15 kJ/kg) is slightly higher than that of PU1 (305.20 kJ/kg). The analysis attributes this variation to the fixed temperature drop of 100 K and the variable work of the feed pump, suggesting that a smaller and optimized temperature drop between units would result in a more uniform work distribution and greater overall efficiency, albeit with a larger number of PUs.

4.3. Scalability and Practical Application for Marine Propulsion

The final section of the results translates the theoretical kJ/kg values into practical engineering data for ship propulsion.

4.3.1 Power Scaling Methodology: The text establishes a direct relationship between specific work (w_n), the mass flow rate of the thermal working fluid (TWF), and the total thermodynamic volume of the system. Table 7 and Figures 8-13 provide clear guidance for scaling.

4.3.2 Quantitative Scaling Examples: The analysis offers concrete examples of how to scale the system:

4.3.2.1 A system with a TWF flow rate of 1 kg/s and a cycle time of 1 second requires a thermodynamic volume of 4.77 m³ and generates 1.51 MW of power.

4.3.2.2 Increasing the flow rate to 10 kg/s (while maintaining the cycle time at 1 second) increases the volume to 47.7 m³ and the power output to 15.13 MW.

4.3.2.3 For high-power applications, such as large ships, a system with a flow rate of 100 kg/s would occupy 477 m³ and produce a substantial power output of 151.3 MW.

4.3.3 Volume Reduction Strategy: The analysis highlights that these volumes are based on a reference pressure of 20 bar. It concludes that the physical size of the plant can be significantly reduced by operating at higher pressures. For example, increasing the reference pressure to 100 bar would theoretically reduce the required volume by a factor of five (from 477 m³ to approximately 95 m³ for a 151 MW plant), making the system much more viable for installation on a ship.

5. Conclusion

Based on the results obtained from the analysis presented in the previous section of the text, a comprehensive proof of concept, both theoretical and simulation-based, is provided for a self-sustaining marine propulsion system.

The key findings are:

5.1. Demonstrated technical feasibility: The sVsVs cycle and cascaded PGT architecture are computationally validated to generate positive net work.

5.2. Confirmed disruptive principle: The high ratio of contraction to expansion work (approximately 80%) validates the core innovation of generating significant energy from thermal contraction (cooling).

5.3. Achieved self-sufficiency: The calculated positive net output of 1513.41 (kJ/kg-cycle), after considering feedback heat, demonstrates the system's ability to maintain its own operation.

5.4. Defined practical scalability: A clear methodology is provided for scaling the system to megawatt power levels, along with a strategy for managing the plant's physical footprint by increasing the operating pressure. In essence, the analysis argues that the proposed technology goes beyond a theoretical concept and presents a set of engineering data supporting its potential as a viable, fuel-free, and emission-free energy source for the maritime industry. However, the results are based on simulation data and assumed loss factors, implying that the next step would be to validate these findings with a physical prototype.

References

- 1 IRENA – International Renewable Energy Agency: IRENA (2025), Renewable energy statistics 2025, International Renewable Energy Agency, Abu Dhabi. Retrieved from: <https://www.irena.org/Publications/2025/Jul/Renewable-energy-statistics-2025>.
- 2 Ramon Ferreira Garcia. Study of the disruptive design of a thermal power plant implemented by several power units coupled in cascade. Energy Technol. 2023, 2300362 (1-17). Published by Wiley-VCH GmbH. DOI: <https://doi.org/10.1002/ente.202300362>.

- 3 Ramón Ferreiro Garcia. Efficient disruptive power plant-based heat engines doing work by means of strictly isothermal closed processes. *Journal of Advances in Physics* Vol 22 (2024), p 30.53, ISSN: 2347-3487. <https://rajpub.com/index.php/jap/article/view/9587>. DOI: <https://doi.org/10.24297/jap.v15i0.9587>.
- 4 Ramón Ferreiro Garcia. Design study of a disruptive self-powered power plant prototype. *Journal of Advances in Physics* Vol 22 (2024), p 62.92, ISSN: 2347-3487. <https://rajpub.com/index.php/jap/article/view/9596>. DOI: <https://doi.org/10.24297/jap.v22i.9596>.
- 5 Ramón Ferreiro Garcia. Prototyping a Disruptive Self-Sustaining Power Plant enabled to overcome Perpetual Motion Machines. *Journal of Advances in Physics* Vol. 22 (2024), p 141.178, ISSN: 2347-3487. <https://rajpub.com/index.php/jap/article/view/963>. DOI: <https://doi.org/10.24297/jap.v22i.9633>.
- 6 Ramón Ferreiro Garcia. Prototyping Self-Sustaining Power Machines with Cascaded Power Units Composed by Pulse Gas Turbines. *Journal of Advances in Physics* Vol. 22 (2024), p 141.178, ISSN: 2347-3487. <https://rajpub.com/index.php/jap/article/view/9648>. DOI: <https://doi.org/10.24297/jap.v22i.9648>
- 7 Ramón Ferreiro Garcia. Prototyping disruptive self-sufficiency power machines composed by cascaded power units based on thermo-hydraulic actuators. *Journal of Advances in Physics* Vol 22 (2024), p 141.178, ISSN: 2347-3487. <https://rajpub.com/index.php/jap/article/view/9662>. DOI: <https://doi.org/10.24297/jap.v22i.9662>.
- 8 Ramón Ferreiro Garcia. How to violate the first law of thermodynamics with an ASE of Papain and Newcomen before it was stated by Clausius. *JOURNAL OF ADVANCES IN PHYSICS*, 23, 9–27. (2025) <https://doi.org/10.24297/jap.v23i.9706>
- 9 Ramon Ferreiro Garcia. *Power Plants and Cycles: Advances and trends*. Book (2020): ISBN: 9789390431595; DOI:10.9734/bpi/mono/978-93-90431-59-5. <https://www.researchgate.net/publication/347635047> *Power Plants and Cycles Advances and Trends*
- 10 Ramon Ferreiro Garcia. Preliminary design task for prototyping Self-Sustaining Power Machines on Mars using local resources. *Journal of Advances in Physics*, 23, 83-115. (2025) <https://doi.org/10.24297/jap.v23i.9737>
- 11 Ramon Ferreiro Garcia. Prototyping Studies for Self-Sufficient Power Machines with local resources from the Moon. *Journal of Advances in Physics*, 23, 116-146 (2025) <https://doi.org/10.24297/jap.v23i.9747>
- 12 Ramon Ferreiro Garcia. Prototyping Studies for Proposal for Prototyping Disruptive Self-Sufficient Power Engines: Harnessing "Pull" Forces. *Journal of Advances in Physics*, 23, 263-304 (2025) <https://doi.org/10.24297/jap.v23i.9792>
- 13 E. W. Lemmon, M. L. Huber, M. O. McLinden, NIST Reference Fluid Thermodynamic And Transport Properties - REFPROP Version 8.0, User's Guide, NIST, Boulder, CO. 2007.
- 14-23. Ramon Ferreiro Garcia. Improving the design of self-sustaining power plant prototypes through profit optimization. *Journal of Advances in Physics*, 23, 315-335 (2025) DOI: <https://doi.org/10.24297/jap.v23i.9821>.
- 15 Patente: Máquina térmica alternativa regenerativa de doble efecto, de procesos cerrados y abiertos y su procedimiento de operación. "Regenerative double-effect heat engine, with closed and open processes and its operating procedure". Ramon Ferreiro Garcia, Jose Carbia Carril. University of A Coruna. Número de solicitud: P201700181. Accessed at: <https://consultas2.oepm.es/ceo/jsp/busqueda/busqRapida.xhtml?jsessionid=qzBIO1KHmr9+xjw8ggw8YH5X.ConsultasC1>.

- 16 Patent: Planta térmica con máquina de doble efecto, acumuladores térmicos, convección forzada y alimentación térmica reforzada con un ciclo Brayton inverso y procedimiento de operación. Thermal power plant with double-effect machine, thermal accumulators, forced convection and reinforced thermal supply with a reverse Brayton cycle and operating procedure. Jose Carbia Carril. Ramon Ferreiro Garcia, application number P201700667 and publication number 2 696 950 B2. Accessed at: <https://consultas2.oepm.es/ceo/jsp/busqueda/busqRapida.xhtml;jsessionid=MDkG1Ola9BfQrxSilmwxtYIC.ConsultasC2>.
- 17 Patent: Procedimiento de operación de una máquina alternativa de doble efecto con adición y extracción de calor y convección forzada. Operating procedure of a double-acting reciprocating machine with heat addition and extraction and forced convection and operating procedure. Ramon Ferreiro Garcia, Jose Carbia Carril, , application number P201700718 and publication number 2 704 449 B2. Accessed at: <https://consultas2.oepm.es/ceo/jsp/busqueda/busqRapida.xhtml;jsessionid=-wHy58sbfVYQutlYN8s0+JJK.ConsultasC1>.
- 18 Patent: Planta termoeléctrica multi estructural policíclica y procedimientos de operación. "Polycyclic multi-structure thermal power plant and operating procedures". Ramon Ferreiro Garcia, Application number: P202200035 and publication number 2 956 342 B2. Accessed at <https://consultas2.oepm.es/ceo/jsp/busqueda/busqRapida.xhtml;jsessionid=-wHy58sbfVYQutlYN8s0+JJK.ConsultasC1>.
<https://www.researchgate.net/publication/347635047> Power Plants and Cycles Advances and Trends
- 19 Patent: Sistema de transferencia de calor para calentar y enfriar módulos de potencia acoplados en cascada de plantas termoeléctricas y procedimiento de operación. "Heat transfer system for heating and cooling cascade-coupled power modules of thermoelectric plants and operating procedure". Ramon Ferreiro Garcia. Application number: P202400002. Accessed at: <https://consultas2.oepm.es/ceo/jsp/busqueda/busqRapida.xhtml;jsessionid=qzBIO1KHmr9+xjw8ggw8YH5X.ConsultasC1>.
- 20 Patent: Ramon Ferreiro Garcia. Gas turbine operating with baro-thermal pulses and operating procedure. Publication number: ES2851381 A1(06.09.2021), Also published as: ES2851381 B2 (27.07.2022). Applicant: FERREIRO GARCIA, Ramón (100.0%) (ES). IPC: F02C3/02 (2006.01). <https://consultas2.oepm.es/InvenesWeb/faces/busquedaInternet.jsp;jsessionid=MDE3o-JscfQB7FbFuhlvN2mR.srvvarsovia1>.
<https://consultas2.oepm.es/InvenesWeb/detalle?referencia=P202000032>
- 21 R.D. Geertsma, R.R. Negenborn, K. Visser, and J.J. Hopman. Design and control of hybrid power and propulsion systems for smart ships: A review of developments. Applied Energy, 194 (2017) 30–54. DOI: <https://doi.org/10.1016/j.apenergy.2017.02.060>
- 22 Ramon Ferreiro Garcia. Prototyping of self-sustaining propulsion systems for solar system exploration. Journal of Advances in Physics, 24, 9-63 (2026)
DOI: <https://doi.org/10.24297/jap.v23i.9872>.